The American Journal of Pathology, Vol. 188, No. 3, March 2018

The American Journal of
PATHOLOGY
ajp.amjpathol.org

IMMUNOPATHOLOGY AND INFECTIOUS DISEASES

Late Disseminated Lyme Disease

Associated Pathology and Spirochete Persistence Posttreatment in Rhesus Macaques

Nicholas A. Crossland,*† Xavier Alvarez,‡ and Monica E. Embers*†

From the Divisions of Bacteriology, Parasitology,† and Comparative Pathology,‡ Tulane National Primate Research Center, Tulane University Health Sciences, Covington, Louisiana*

Accepted for publication November 16, 2017.

Address correspondence to Monica E. Embers, Ph.D., Tulane National Primate Research Center, Tulane University Health Sciences, 18703 Three Rivers Rd., Covington, LA 70433. E-mail: members@tulane.edu.

Nonhuman primates currently serve as the best experimental model for Lyme disease because of their close genetic homology with humans and demonstration of all three phases of disease after infection with *Borrelia burgdorferi*. We investigated the pathology associated with late disseminated Lyme disease (12 to 13 months after tick inoculation) in doxycycline-treated (28 days; 5 mg/kg, oral, twice daily) and untreated rhesus macaques. Minimal to moderate lymphoplasmacytic inflammation, with a predilection for perivascular spaces and collagenous tissues, was observed in multiple tissues, including the cerebral leptomeninges, brainstem, peripheral nerves from both fore and hind limbs, stifle synovium and perisynovial adipose tissue, urinary bladder, skeletal muscle, myocardium, and visceral pericardium. Indirect immunofluorescence assays that combined monoclonal (outer surface protein A) and polyclonal antibodies were performed on all tissue sections that contained inflammation. Rare morphologically intact spirochetes were observed in the brains of two treated rhesus macaques, the heart of one treated rhesus macaque, and adjacent to a peripheral nerve of an untreated animal. *Borrelia* antigen staining of probable spirochete cross sections was also observed in heart, skeletal muscle, and near peripheral nerves of treated and untreated animals. These findings support the notion that chronic Lyme disease symptoms can be attributable to residual inflammation in and around tissues that harbor a low burden of persistent host-adapted spirochetes and/or residual antigen. *(Am J Pathol 2018, 188: 672–682; https://doi.org/10.1016/j.ajpath.2017.11.005)*

The first well-documented indication of Lyme disease (LD) in the United States occurred in the early 1970s, manifesting as an outbreak of asymmetric large joint oligoarthritis in the community of Lyme, Connecticut.[1,2] Steere et al[1] speculated that the tight geographic clustering in a sparsely populated, heavily wooded area and the peak incidence in the summer and early fall months were suggestive of an arthropod-vectored disease. This hypothesis was later confirmed by Burgdorfer et al,[3] who isolated *Treponema*-like spirochete bacteria from adult *Ixodes dammini* (*scapularis*) ticks on Shelter Island, New York. The spirochetes were named *Borrelia burgdorferi* after their discoverer.[3] Currently, LD is known to be caused by multiple closely related genospecies classified within the *B. burgdorferi* sensu lato complex, representing the most common tickborne human disease in the Northern Hemisphere.[4,5] Although approximately 30,000 physician-reported cases occur annually in the United States, the annual incidence has been estimated to be 10-fold higher by the Centers for Disease Control and Prevention.[6]

Current antibiotic therapy guidelines outlined by the Infectious Disease Society of America (IDSA) are successful in the treatment of LD for most patients with LD,

Supported by Louisiana Center of Biomedical Research Excellence in Experimental Infectious Disease Research grant 2P20-RR020159-08 (M.E.E.), Tulane National Primate Research Center NIH base grant 5 P51 OD 011104-56, the Bay Area Lyme Foundation (M.E.E.), and the Steven and Alexandra Cohen Foundation (M.E.E.).

Disclosures: None declared.

https://doi.org/10.1016/j.ajpath.2017.11.005

especially when administered early in disease immediately after identification of erythema migrans (EM).[7] Although EM is considered an early localized reaction and clinical hallmark of LD, EM is not pathognomonic and is not observed in 100% of cases,[8] which results in delays in treatment that range from weeks to months after initial exposure. Chronic subjective symptoms (ie, musculoskeletal pains, cognitive dysfunction, radicular pain, paresthesia, dysesthesia, and/or fatigue) and, less commonly, objective clinical signs (ie, arthritis and/or neurologic deficits), which remain for months to years after completion of recommended antibiotic therapy in patients with well-documented LD, are classified into posttreatment LD syndrome (PTLDS).[9]

Considerable confusion and controversy exist about the frequency and cause of PTLDS and even about its existence. Although progress has been made in the development of a standard case definition for PTLDS, the absence of an available test to confirm or rule out persistence of *B. burgdorferi* adds to the quandary.[9,10] We and others have speculated that decreased efficacy of antibiotic treatment in LD may be attributed to several causes, including the following: i) host-adapted spirochetes that persist in the tissues, probably in small numbers, inaccessible or impervious to antibiotics; ii) inflammatory responses to residual antigens from dead organisms; iii) residual tissue damage after pathogen clearance; and/or iv) autoimmune responses, possibly elicited by antigenic mimicry.[11–13] Experimental studies on immunocompetent mice, dogs, and rhesus macaques have provided evidence of the persistence of *B. burgdorferi* spirochetes subsequent to antibiotic treatment in the form of residual spirochetes detected within tissue by immunofluorescent assay (IFA) and PCR and recovered by xenodiagnoses.[13–17] These findings support the role of persistent, host-adapted *B. burgdorferi* spirochetes in the etiology of PTLDS, yet these spirochetes may be difficult to impossible to regrow by current tissue culture methods after prolonged infection. This experimental dilemma is paralleled by clinical observations of negative culture results in confirmed cases of Lyme carditis that resulted in sudden cardiac death, in which morphologically intact spirochetes were readily observed in affected heart sections by immunohistochemistry.[18]

We used tick-mediated inoculation of *B. burgdorferi* strain B31 into nonhuman primates (NHPs), followed by doxycycline treatment directed toward disseminated disease, thus aiming to accurately model chronic LD of humans whose treatment is delayed. It was hypothesized that late-stage disseminated LD in rhesus macaques infected by tick bite would display residual microscopic pathologic findings in a variety of different tissues previously indicated in natural and experimental LD [ie, peripheral nervous system, central nervous system, heart, skeletal muscle, and joint-associated tissues] and that this pathologic finding would be directly associated with residual spirochetal antigens and/or viable host-adapted spirochetes.

Materials and Methods

Ethical Statement

Practices in the housing and care of animals conformed to the regulations and standards of the Public Health Service Policy on Humane Care and Use of Laboratory Animals and the Guide for the Care and Use of Laboratory Animals.[19] The Tulane National Primate Research Center (Animal Welfare Assurance A4499-01) is fully accredited by the Association for the Assessment and Accreditation of Laboratory Animal Care—International. The Institutional Animal Care and Use Committee of the Tulane National Primate Research Center approved all animal-related protocols, including the infection, treatment, and tick-feeding procedures used with NHPs. All animal procedures were overseen by veterinarians and performed by veterinarians or trained staff. Euthanasia was conducted by anesthesia with ketamine hydrochloride (10 mg/kg) followed by an overdose with sodium pentobarbital. This method is consistent with the recommendation of the American Veterinary Medical Association guidelines.

Animals, Inoculations, and Treatment

Ten male rhesus macaques of Indian origin, 3 to 4 years of age, were fed on by *I. scapularis* nymphal ticks that harbored *B. burgdorferi*. To ensure infection, *I. scapularis* nymphs were fed the spirochetes via capillary tubes (from a mid-log phase culture of strain B31) as previously described.[20,21] Ten *B. burgdorferi*—containing nymphs were placed on the backs of all 10 monkeys in a tick containment device, as previously described.[13,21] Ticks were allowed to feed for 4 days to transmit infection. A recently developed five-antigen Bioplex assay was used to detect and quantify antibody responses.[22] Skin biopsy samples were also used to verify infection by culture and PCR.[13] Half of the animals produced positive skin biopsy cultures, and 8 of 10 were PCR positive. At 4 months after inoculation, half (five) of the NHPs received antibiotic treatment, consisting of 5 mg/kg of oral doxycycline twice per day. The treatment lasted 28 days, and no instances of nonadherence were observed. With the exception of IK14 (0.1 to 0.26 μg/mL), the serum values obtained at 12 hours after dosing (0.98 to 1.87 μg/mL) were above or consistent with expected trough values derived from our previous pharmacokinetic study.[23] Blood was drawn at day 0, every 2 weeks for the first 5 months, then monthly thereafter. Further details of the serologic responses, serum doxycycline concentrations, and detection of persistent spirochetes by multiple methods are discussed in Embers et al.[24] Necropsies were performed at 8 to 9 months after the cessation of treatment (12 to 13 months after inoculation).

Histopathologic Analysis and Microscopic Grading

Representative sections of brain (cerebrum, cerebellum, and brainstem), dura mater, spinal cord (cervical, thoracic,

lumbar, and sacral) and associated dorsal root ganglia, peripheral nerves (radial, ulnar, tibial, and sural), joint-associated tissues (shoulder and stifle), heart, skeletal muscle, lung, spleen, axillary and mesenteric lymph nodes, and urinary bladder were collected from each animal, fixed in Z-fix (Anatech Ltd., Battle Creek, MI) for 24 to 48 hours, embedded in paraffin, sectioned at 5 μm, and stained with hematoxylin and eosin. Peripheral nerves were mistakenly not collected for routine histopathologic analysis from one untreated animal (IP67). Hematoxylin and eosin−stained sections were evaluated by a light microscope and imaged with a digital camera. Two independent veterinary pathologists (N.A.C. and Dr. Peter J. Didier) evaluated tissues. Initially, all tissues were evaluated to determine the variability and severity of pathologic findings from all samples, with the pathologists blinded to the treatment groups (N.A.C. and Dr. Peter J. Didier). Tissues that were observed to contain pathologic findings were used as a roadmap for subsequent immunofluorescent staining to identify *B. burgdorferi*. On the basis of the range of lesions observed, an ordinal scoring system ranging from 0 to 3 was developed to classify inflammatory profiles. A zero score indicated that inflammation was not observed, a score of 1 indicated minimal localized lymphoplasmacytic inflammation, a score of 2 indicated minimal lymphoplasmacytic inflammation with multifocal distribution or mild inflammation with focal or multifocal distribution, and a score of 3 indicated moderate lymphoplasmacytic inflammation. A score of 3 was always associated with a multifocal distribution. Control tissues were obtained from four male, age-matched, rhesus macaques. Two of these animals were control, sham (intrathecal) inoculated subjects from a previous Lyme neuroborreliosis study.[25] The additional two rhesus macaques were humanely euthanized because of intractable chronic diarrhea and had not previously been in an LD study. Statistical analyses were conducted with GraphPad Prism software version 6 (GraphPad Software, Inc., San Diego, CA).

Detection of *B. burgdorferi* by Indirect IFA

An identical set of tissues as previously described in *Histopathologic Analysis and Microscopic Grading* were also collected at necropsy (in addition to peripheral nerves from IP67), placed in PolyCon containers that contained OCT medium, frozen immediately in a dry ice/methanol bath, and then stored at −80°C. Only sections with inflammation confirmed through histopathologic analysis were evaluated by IFA. Frozen samples were processed by cryosectioning (at 15 μm), with four to eight sections (60 to 120 μm) of each tissue examined, depending on how much tissue could fit onto four slides. All incubations were performed at room temperature, and all wash steps were performed for 10 minutes while gently rocking in Kopplin jars unless otherwise stated. Frozen sections were thawed for 20 minutes, followed by submersion in 4% paraformaldehyde for 20 minutes at 4°C. Slides were then washed twice with 1× phosphate-buffered saline (PBS), and tissues were circled by a wax pen. Next, tissues were submerged in 100 mmol/L glycine diluted in PBS, 0.2% fish skin gelatin (FSG), and 0.1% Triton X-100 to neutralize residual paraformaldehyde. Before blocking of slides, two additional wash steps were performed with PBS, FSG, and Triton X-100 and PBS and FSG, respectively. In a dark humidified staining box, the slides were blocked with 10% normal goat serum, PBS, and FSG for 1 hour. Blocking agent was gently removed from the slides by tapping the glass edge onto a paper towel immediately before the addition of primary antibodies. Two primary antibodies were used simultaneously, which included a rabbit polyclonal anti−*B. burgdorferi* (derived from a hyperimmunized rabbit 6 weeks after inoculation with *in vitro* propagated *B. burgdorferi* strain B31[26]) and an anti−outer surface protein A (OspA) monoclonal IgG hybridoma supernatant [CB10, kindly provided by Dr. Jorge Benach (Stony Brook University School of Medicine, Stony Brook, NY)]. Polyclonal rabbit serum was diluted 1:300, and the monoclonal antibody hybridoma supernatant was diluted 1:40 in normal goat serum, PBS, and FSG, with approximately 300 μL added to each tissue section, followed by a 1-hour incubation. Slides were washed twice with PBS, FSG, and Triton X-100 and a final rinse with PBS and FSG. Tissue sections were then incubated for 1 hour with 300 μL of secondary antibodies conjugated to fluorescent dyes diluted 1:1000 in normal goat serum, PBS, and FSG (Goat Anti-Rabbit IgG-Alexa Fluor 488, catalog number A32731 and Goat Anti-Mouse IgG Alexa Fluor 568, catalog number A-11004; Thermo Fisher Scientific, Waltham, MA). Three additional wash steps identical to those performed after incubation with primary antibodies were performed. After the final wash, slides were partially dried by tapping the glass edge onto a paper towel and immediately mounted with an in-house prepared antiquenching glycerol-based mounting media, coverslipped, and allowed to sit overnight. Pre-inoculation serum from the rabbit used to obtain hyperimmune serum was used in the primary antibody step (diluted 1:300) to serve as a negative control, which displayed neither red nor green fluorescence when applied to positive control slides. Brain sections from a rhesus macaque that were cut to 15 μm and incubated with *B. burgdorferi* strain B31 *ex vivo* served as a positive control.[27] In addition, the IFA was performed on frozen sections that originated from one of the control animals that was euthanized because of intractable diarrhea. For this control animal, IFA was performed on an identical set of tissues as examined in experimental animals. Spirochetes were not observed in any of control animal sections examined. Imaging was performed with a Leica DMi8 confocal microscope equipped with three lasers (Leica Microsystems, Wetzlar, Germany) using a 63× objective, with a resolution of 1024 × 1024 pixels. An additional 2× amplification was applied with Leica LAS X software version 10 (Leica Microsystems Inc., Buffalo Grove, IL) when appropriate. Start and stop depths were assigned for

each image, allowing for maximization by z stacking of images. Frame average was set at 2. Laser intensity was optimized on positive control tissues and remained constant for all test specimens. Volocity three-dimensional image analysis software version 6.3.1 (Perkin Elmer, Waltham, MA) was used to render images for three-dimensional display and angle rotation. Adobe Photoshop CC 2017 and InDesign 2017 software (Adobe Systems, San Jose, CA) were used to process and assemble the images and figures, respectively. When made, adjustments to brightness, contrast, or color balance were applied to the whole image.

RNAscope ISH Procedure

RNAscope is commercially available from Advanced Cell Diagnostics (Newark, CA).[28] RNA in situ hybridization (ISH) was performed using the RNAscope Multiplex Fluorescent Detection Kit version 2 according to the manufacturer's guidelines. In brief, for each specimen investigated, three serial, 15-μm fresh-frozen sections were fixed in 4% paraformaldehyde at 4°C for 15 minutes and dehydrated in a series of ethanol washes. Slides were then treated with RNAscope hydrogen peroxide for 10 minutes and RNAscope protease IV for 30 minutes at room temperature. A different probe was used for each of the three serial sections, which included the following: *B. burgdorferi* probe (23S rRNA transcript, catalog number 468211), positive probe [rhesus macaque peptidyl-prolyl *cis-trans* isomerase (PPIB), catalog number 457711] and negative probe (*Bacillus subtillis dapB*, catalog number 320871). Each of the probes were designed and synthesized by Advanced Cell Diagnostics. After the amplification process, tyramide signal amplification cyanine 5 was used to visualize the ISH reaction (Perkin Elmer; catalog number SAT705A001 EA). Tissues were mounted with a glycerol-based antiquenching media prepared in house, coverslipped, and allowed to sit overnight. Imaging was performed with a Leica DMi8 confocal microscope as previously described in *Detection of B. burgdorferi by Indirect IFA*.

Results

For the sake of continuity, histopathologic, IFA, and ISH results are described together by organ system. When stated, observed fluorescence indicates a reaction with rabbit hyperimmune *B. burgdorferi* polyclonal antibodies (Figure 1A) or mouse hybridoma-derived anti-OspA monoclonal antibodies (Figure 1B). Given the sectioning at 15 μM, spirochetes can be observed as full length in the lateral plane, as cross sections, or as fragments (Figure 1, A and B). A merged image of green and red channels is provided from *ex vivo* brain tissue cultured with *B. burgdorferi* strain B31 *in vitro* (Figure 1C). A summary of results can be found in Table 1. No significant gross findings were observed in any of the experimental animals.

Nervous System

Minimal and focal lymphoplasmacytic inflammation of the central nervous system was observed in two animals, both of which were treated with doxycycline (IH11 and IH22). In IH11, inflammation was observed in the leptomeninges overlying a section of temporal cerebral cortex (Figure 1D, Supplemental Figure S1), whereas inflammation in IH22 was characterized by perivascular inflammation of the brainstem adjacent to the fourth ventricle (Figure 1E). Green fluorescent *B. burgdorferi*–specific staining was detected free within the neuropil of both these animals (Figure 1, F and G) and was not directly associated with the minimal inflammation observed histologically. Of all the sections examined in this study, the greatest density of morphologically intact spirochetes was observed in the cerebrum of IH11, with up to six spirochetes observed in a single high-powered field (63×). Because of the limited number of animals tested, the proportion of monkeys that exhibited inflammation in the CNS between the treated (two of five monkeys) and untreated group (zero of five monkeys) was not significantly different (Fisher's exact test, two-tailed, $P = 0.444$). When IFA was multiplexed with RNA ISH (Supplemental Figure S2), colocalization of *B. burgdorferi* immunofluorescence was not observed with a 23S rRNA *B. burgdorferi* probe (Supplemental Figure S1). Minimal localized lymphoplasmacytic choroiditis was observed in one of the four control animals; however, no inflammation was observed in a representative section of cerebrum, cerebellum, brainstem, spinal cord, or dura mater from untreated or control animals (Table 1).

Peripheral nerves contained minimal to moderate lymphoplasmacytic inflammation with a predilection for collagen-rich epineurium and perivascular spaces (Figure 1, H–J). Inflammation was observed in five of nine NHPs (56%) irrespective of treatment group, with three of four untreated (75%) and two of five doxycycline-treated (40%) animals affected. Grade 3 inflammation scores (moderate) were observed in two untreated animals, and multiple peripheral nerves were affected in all three untreated animals (Table 1). For all animals, inflammation was reserved to perineural tissue. No inflammation was observed within nerve fibers, and there was no evidence of axonal degeneration that would have been supported by the presence of dilated myelin sheaths or axonal spheroids. The frequency of lymphoplasmacytic perineuritis (in decreasing order) involved the left sural ($n = 3/9$), right ulnar ($n = 3/9$), left tibial ($n = 1/9$), right tibial ($n = 1/9$), right sural ($n = 1/9$), right median ($n = 1/9$), left median ($n = 1/9$), cervical spinal nerve ($n = 1/9$), and lumbar spinal nerve ($n = 1/9$). No inflammation was observed in dorsal root ganglia from any of the animals, and there was no histologic evidence of neuronal degeneration or necrosis (ie, chromatolysis and shrunken angular hypereosinophilic neurons, respectively). Peripheral nerves for IP67 (untreated) were mistakenly not collected for hematoxylin and eosin and thus were unavailable for routine

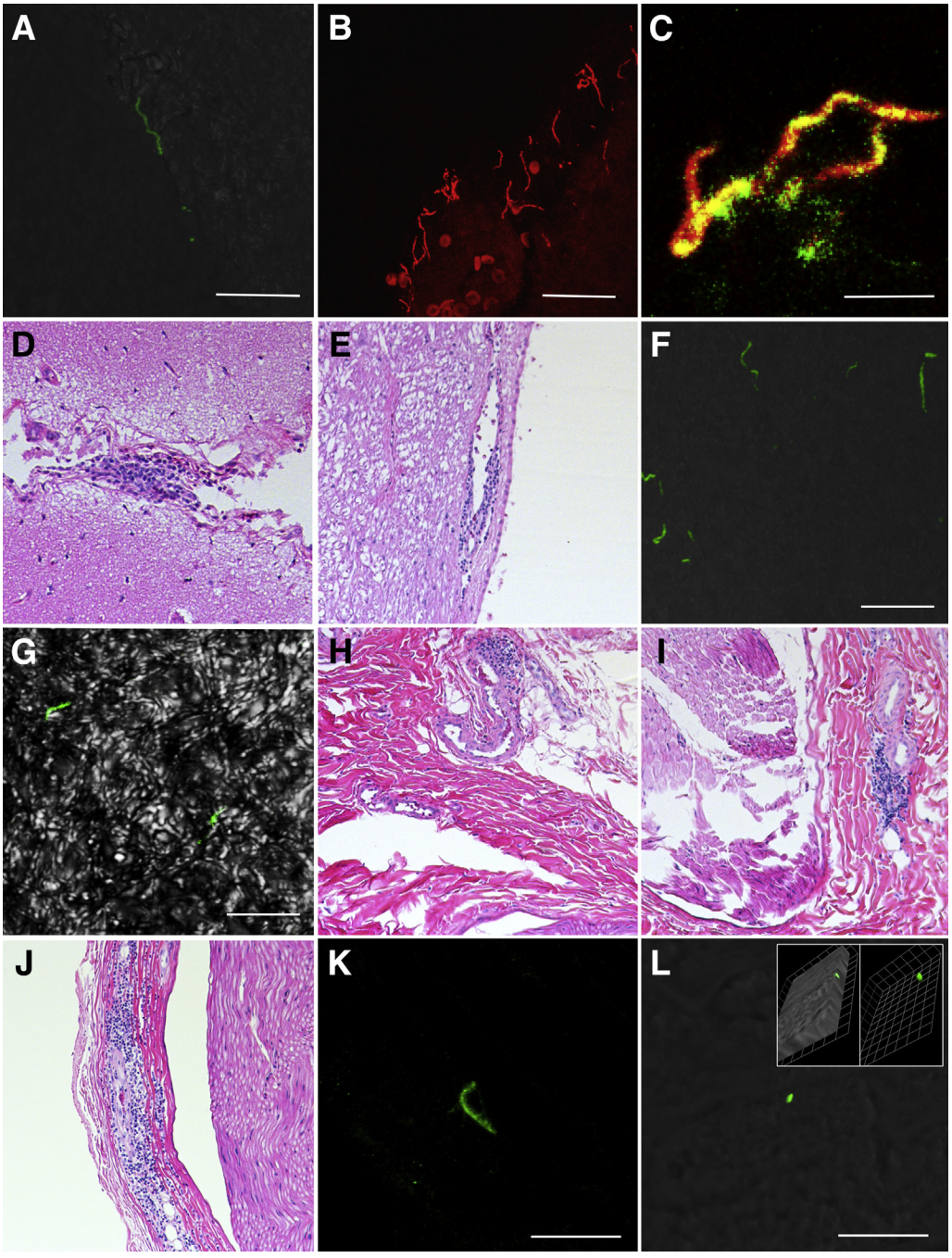

Figure 1 Histologic characterization and localization of *Borrelia burgdorferi* within doxycycline and untreated rhesus macaques with late disseminated Lyme disease. **A:** *B. burgdorferi* polyclonal positive control immunofluorescence assay (IFA); rabbit *B. burgdorferi* hyperimmunized polyclonal (primary) and goat anti-rabbit IgG Alexa Fluor 488 (secondary) antibodies. Green fluorescence of a morphologically intact spirochete. **B:** *B. burgdorferi* monoclonal positive control IFA; mouse outer surface protein A monoclonal (primary) and goat anti-mouse IgG Alexa Fluor 568 (secondary) antibodies. Red fluorescence of morphologically intact spirochetes. **C:** Green and red confocal channels merged, with yellow indicating colocalization of monoclonal and polyclonal antibodies from positive control tissue. **D:** Cerebrum (IH11 doxycycline treated); leptomeninges are focally expanded by minimal localized lymphoplasmacytic inflammation. **E:** Brainstem (IH22 doxycycline treated); minimal localized lymphoplasmacytic perivascular cuffing adjacent to the fourth ventricle. **F:** Green fluorescence illustrates six variably sized morphologically intact spirochetes within the cerebral neuropil. **G:** Green fluorescence reveals two morphologically intact spirochetes within the brainstem neuropil; differential interference contrast (DIC) applied to enhance contrast. **H:** Ulnar nerve (IK66 doxycycline treated); minimal localized lymphoplasmacytic perivascular cuffing adjacent to the epineurium. **I:** Sural nerve (IL75 untreated); mild localized lymphoplasmacytic perivascular cuffing within the epineurium. **J:** Ulnar nerve (IP55 untreated); moderate focally extensive lymphoplasmacytic inflammation radiating outward from a vessel and dissecting neighboring epineurium. **K:** Green fluorescence illustrates a morphologically intact spirochete within the right tibial epineurium (IP55 untreated). **L:** Localized green fluorescence adjacent to left ulnar axonal nerve fibers (IP67 untreated); DIC image applied to enhance contrast. Three-dimensional imaging in **inset** shows the cylindrical shape with convex end of the structure, indicating that this may be a cross section at the end/pole of the spirochete; 1 unit = 1.88 μm. Scale bars: 20 μm (**A**, **B**, **F**, and **K**); 10 μm (**C**, **G**, and **L**). Original magnification: ×10 (**D**, **E**, and **H**–**J**); ×63 (additional ×2 amplification applied with Leica LAS X software when appropriate; **A**–**C**, **F**, **G**, **K** and **L**).

Table 1 Summary of Histopathologic Findings in *Borrelia burgdorferi* Tick-Infected Rhesus Macaques

Group	Age, y	Peripheral nerves	Heart/pericardium	Brain/leptomeninges	Urinary bladder	Skeletal muscle	Stifle joint
Untreated							
IP55	3.73	3* (green)†	0/0	0	2	0	0
IP67	3.89	NE (green)†	0/0	0	0	0	0
IN16	3.83	0	2/0	0	3	0	1
IL75	4.06	3*	0/0	0	2 (red)†	0	0
IN05	4.11	2*	1/0	0	2	0	0
Ratio (%)	NA	3/4 (75)	2/5 (40)	0/0 (0)	4/5 (80)	0/5 (0)	1/5 (20)
Treated							
IH11	3.97	2*	1/0	1 (green)†	3	0	2
IK66	3.92	1	1/0	0	2	2 (green and red)†	0
IK14	4.09	0	2/0 (red)†	0	2	0	0
IL09	4.07	0	0/0	0	2	0	1 (red)†
IH22	4.18	0	2/2	1 (green)†	0	0	0
Ratio (%)	NA	2/5 (40)	4/5 (80)	2/5 (40)	4/5 (80)	1/5 (20)	2/5 (40)
Controls							
HT73	4.16	0	0	0	2	0	NE
IK20	3.99	0	0	0	NE	NE	NE
KB40	5.17	1	0	1	1	0	0
IH80	7.59	0	3 (marked fibrosis)	0	2	0	1
Ratio (%)	NA	1/4 (25)	1/4 (25)	1/4 (25)	3/3 (100)	0/3 (0)	1/2 (50)

*Multiple nerves affected simultaneously.

†Positive by immunofluoresence. Red represents detection by anti—outer surface protein A monoclonal antibodies; green represents detection by rabbit anti-*Borrelia* polyclonal antibodies.

NA, not applicable; NE, not examined.

histopathologic evaluation; however, sections were collected from frozen specimens and immunofluorescence was performed. Green fluorescent staining for *B. burgdorferi* was observed in untreated animals IP55 (Figure 1, K) and IP67 (Figure 1, L), represented by a morphologically intact spirochete in the former. Minimal localized perivascular lymphoplasmacytic perineuritis that affected the right sural nerve was observed in one of the four control animals. Positive *B. burgdorferi*—specific fluorescence was not observed in representative sections of CNS and peripheral nervous system tissues derived from control animals.

Heart

Minimal to mild lymphoplasmacytic inflammation of the myocardial interstitium (Figure 2A), pericardium (Figure 2B), or combination therein was observed in 60% of NHPs irrespective of treatment groups, with two of five untreated (40%) and four of five doxycycline-treated (80%) NHPs affected. Lymphoplasmacytic inflammation of the pericardium was only observed in animals with myocardial involvement. Inflammation was not associated with histologic evidence of myocardial degeneration, necrosis, and/or fibrosis. A single morphologically intact spirochete, as indicated by positive red immunofluorescence (Figure 2C), was observed in the myocardium of one treated animal (IK14). Moderate lymphoplasmacytic myocarditis was observed in one of the four control animals; however, this animal also had marked myocardial fibrosis, which was not observed in any of the other experimental or control animals. This animal also had evidence of systemic illness ultimately attributed to severe chronic intractable colitis and was the oldest of all the control animals used. No immunofluorescence was observed in representative sections of myocardium and pericardium derived from control animals.

Skeletal Muscle

Random sections of arm and thigh skeletal muscle were obtained from each animal. Of all the animals examined, mild, multifocal lymphoplasmacytic inflammation was observed in one doxycycline-treated animal (IK66) (Figure 2D), with concurrent positive fluorescence in the form of antigen co-localized with both *B. burgdorferi*—specific antibodies observed (Figure 2, E—G). When consecutive layers of confocal imagining were combined into three dimensions, the antigen was in the form of a cylinder, indicating that this was indeed a cross section of the spirochete (Supplemental Video S1). In this animal, inflammation was characterized by perivascular and interstitial distribution but was not associated with concurrent histologic evidence of rhabdomyocyte degeneration, necrosis, and/or fibrosis. No inflammation or positive fluorescence was observed in representative sections of skeletal muscle derived from control animals.

Synovium

A total of three animals exhibited minimal to mild lymphoplasmacytic inflammation that affected joint-associated

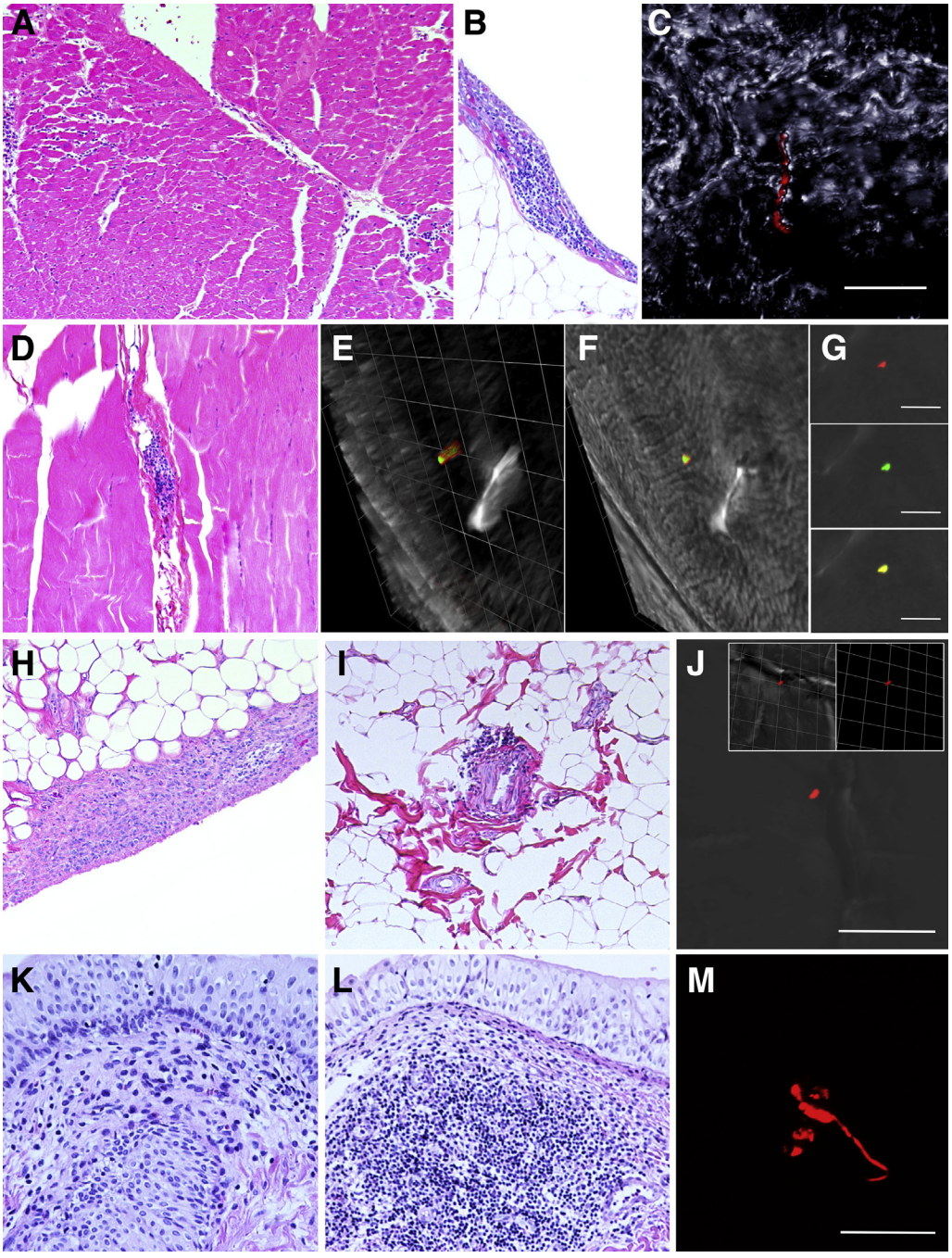

Figure 2 Histologic characterization and localization of *Borrelia burgdorferi* within doxycycline and untreated rhesus macaques with late disseminated Lyme disease. **A:** Heart (IH22 doxycycline treated); mild multifocal lymphoplasmacytic interstitial inflammation. **B:** Visceral pericardium (IH22 doxycycline treated); localized mild lymphoplasmacytic inflammation. **C:** Heart (IK14 doxycycline treated); red fluorescence of a morphologically intact spirochete within myocardial interstitium; differential interference contrast (DIC) image applied to enhance contrast. **D:** Skeletal muscle (IK66 doxycycline treated); mild localized lymphoplasmacytic interstitial inflammation. **E**–**G:** Red, green, and merged images illustrate localized interstitial fluorescence within the skeletal muscle (IK66); DIC image applied to enhance contrast. **E:** Three-dimensional imaging reveals the cylindrical morphologic features of the dual-stained specimen, with the DIC partially removed, indicating that this is a cross section of a spirochete; 1 unit = 6.17 μm. **F:** DIC added back to the three-dimensional rotated view. **G:** Red, green, and merged immunofluorescent staining of *B. burgdorferi* within the tissue. **H:** Stifle synovium (IH11 doxycycline treated); mild lymphoplasmacytic inflammation infiltrating hyperplastic synovial epithelium. **I:** Stifle perisynovial adipose tissue (IL09 doxycycline treated); minimal localized lymphoplasmacytic perivascular cuffing. **J:** Localized red fluorescence in perisynovial adipose tissue (IL09 doxycycline treated). Three-dimensional imaging in **inset** shows cylindrical shape of the structure, indicating that this may be a cross section of the spirochete; 1 unit = 6.17 μm. DIC image applied to enhance contrast. **K:** Urinary bladder; the lamina propria is infiltrated by mild lymphoplasmacytic inflammation. **L:** Urinary bladder; a discrete lymphoid nodule expands the lamina propria. **M:** Red fluorescent staining reveals an object with spirochete morphologic features and/or associated antigen within the lamina propria of the urinary bladder (IL75 untreated). Scale bars: 20 μm (**C** and **M**); 10 μm (**E**–**G**, and **J**). Original magnification: ×10 (**A**, **B**, **D**, **H**, **I**, **K**, and **L**); ×63 (additional ×2 amplification applied with Leica LAS X software; **C**).

structures, all of which involved the stifle joints. In two animals, one untreated (IN16) and one treated (IH11), inflammation was present within the synovial membrane (Figure 2H). These animals also had concurrent synovial epithelial hyperplasia that ranged from minimal to mild. One doxycycline-treated animal (IL09) contained minimal perivascular lymphoplasmacytic inflammation in the perisynovial adipose tissue (Figure 2I). Positive red fluorescent anti-OspA staining of what appears to be a cross section of the spirochete (Figure 2J) was observed in one doxycycline-treated animal (IL09). Joint synovium was not collected from Lyme neuroborreliosis control animals; however, synovium (bilateral stifle and shoulder joints) was collected from two animals with chronic treatment-resistant diarrhea with no gross evidence of joint disease. Minimal localized lymphoplasmacytic inflammation was observed in the synovium of one animal, but synovial hyperplasia and perivascular inflammation of perisynovial adipose tissue were not observed and no positive fluorescence was observed.

Additional Tissues

Other tissues examined histologically included axillary and mesenteric lymph nodes, urinary bladder, lung, and spleen. Findings in these tissues were similar among treatment groups and control tissues. Thus, findings were interpreted as nonspecific, and their overall significance was indeterminate. Reactive lymphoid hyperplasia was observed to some extent in all lymph nodes examined (not shown) and was more prominent in mesenteric lymph nodes, ranging from minimal to moderate. The latter was characterized by prominent cortical lymphoid follicles with germinal centers, variable degrees of sinus histiocytosis, and anthracosis in the case of axillary lymph nodes. Minimal to mild lymphoplasmacytic inflammation was observed within the lamina propria of the urinary bladder (Figure 2K), with rare discrete formation of lymphoid follicles (Figure 2L) observed irrespective of treatment groups and control specimens. Because *B. burgdorferi* has previously been cultured from the urinary bladders of experimental animals[29] and all animals had some degree of inflammation, IFA was performed on all study animals, with one positively identified spirochete and/or spirochetal antigen observed in untreated animal IL75 (Figure 2M). No positive fluorescence was detected in control specimens. Splenic white pulp displayed minimal to mild lymphoid hyperplasia irrespective of treatment group and in control specimens. Lastly, lung sections from both treatment groups and control animals displayed minimal to mild peribronchiolar and perivascular lymphoplasmacytic inflammation, with mild anthracosis, and mild alveolar histiocytosis (not shown). One untreated animal (IH22) had multifocal, mild, patchy granulomatous interstitial inflammation. Special stains and/or bacterial culture were not performed on this case, but intralesional birefringent foreign material appeared to be associated with the granulomatous inflammation, suggestive of a foreign-body response.

Discussion

Posttreatment LD remains a poorly understood syndrome, occurring in an estimated 10% to 20% of humans treated under current IDSA guidelines.[30] Multiple randomized, placebo-controlled studies that evaluated sustained antimicrobial therapy concluded that there is no benefit in alleviating patients' symptoms and indicated that long-term antibiotic therapy may even be detrimental to patients because of potential associated complications (ie, catheter infection and/or clostridial colitis).[31–33] A model of late disseminated borreliosis was chosen over other stages of disease because of a general consensus that most patients treated for LD during early localized LD recover from the infection.

In this study, we found microscopic pathologic findings that range from minimal to moderate in multiple different tissues previously reported to be involved with LD, including the nervous system (central and peripheral), heart, skeletal muscle, joint-associated tissues, and urinary bladder 12 to 13 months after tick inoculation of rhesus macaques by *B. burgdorferi* strain B31. On the basis of histomorphologic findings, inflammation consisted predominantly of lymphocytes and plasma cells, with rare scattered histiocytes. A predilection for perivascular spaces and an affinity for collagenous tissue was a common theme among examined tissues. Furthermore, in rare instances, morphologically intact spirochetes were observed in inflamed brain and heart tissue sections from doxycycline-treated animals. Because no inflammation was observed in the CNS of untreated animals, we cannot definitely determine whether spirochetes were also present in those cases. The ISH/IFA multiplex protocol was successfully optimized on *ex vivo* rhesus macaque brain tissues cultured with *B. burgdorferi* strain B31 (Supplemental Figure S2, A–D). However, colocalization of the *B. burgdorferi* 23S rRNA probe was not observed in any of the sections of experimental inoculated animals found to harbor rare persistent spirochetes (Supplemental Figure S1). Previous *in vitro* work has found large decreases in *B. burgdorferi* rRNA levels when in a stationary phase of growth despite most spirochetes remaining viable[34] and may help afford an explanation for these results when compared with validation results of the multiplex assay in the positive control tissues. In addition, the control specimens were fixed before freezing, and the experimental specimens were not. The possibility that the spirochetes were intact but dead also exists, although this may be unlikely given the precedence for viable but noncultivable *B. burgdorferi* after treatment[16] and the rapid clearance of dead spirochetes in a murine model.[35] Future studies would benefit from the use of genes associated with dormancy for ISH to determine whether rare host-adapted spirochetes present in late disseminated LD are transcriptionally active.

The doxycycline dose used in this study (5 mg/kg) was based on a previous pharmacokinetic analysis of oral doxycycline in rhesus macaques proven to be comparable to

levels achieved in humans and was meant to mimic treatment of disseminated LD.[23] The most relevant property of a bacteriostatic antibiotic such as doxycycline is the minimum inhibitory concentration. With the exception of IK14, trough levels of doxycycline were found to be >0.8 μg/mL, which is above the minimum inhibitory concentration for the *B. burgdorferi* strain used in this study.[23] These results indicate that the dosage used in this study is sufficient in establishing an efficacious ratio of area under the concentration-time curve from 0 to 24 hours to minimum inhibitory concentration, which represents the best indicator of doxycycline efficacy. Although current IDSA guidelines recommend i.v. ceftriaxone (2 g per day for 30 days) over oral doxycycline for treatment of neuroborreliosis, a randomized clinical trial failed to show any enhanced efficacy of i.v. penicillin G to oral doxycycline for treatment of Lyme neuroborreliosis (no treatment failures were reported in this study of 54 patients). Although we did not measure the doxycycline levels in the cerebrospinal fluid, they have been found to be 12% to 15% of the amount measured in serum,[36] suggesting that higher doses may be needed to combat neuroborreliosis. The treatment protocol began in the early disseminated phase,[37] without objective indications of neurologic impairment in the primates, and therefore followed the recommended course of doxycycline for 28 days. In the context of another study, these findings suggest that the antibiotic protocol should not represent a major limitation.[38]

B. burgdorferi spirochetes are not known to carry any specific genes that function to confer resistance to the recommended antibiotics (tetracyclines and cephalosporins).[39] We and others have found the development of a drug-tolerant persister population when *B. burgdorferi* are treated with antibiotics *in vitro*.[40,41] The adoption of a dormant or slow-growing phenotype likely allows the spirochetes to survive and regrow after removal of antibiotic. Neutrophil calprotectin may also contribute to antibiotic tolerance by inhibiting the growth of *B. burgdorferi* near inflammatory lesions.[42] The basic premise that antibiotic tolerance may be an adaptation of the sophisticated stringent response required for the enzootic cycle by the spirochetes is described in a recent review as well.[43] In 2014, a trailblazing study in mice found a marked decrease in *B. burgdorferi* DNA in the tissues for up to 8 months after antibiotic treatment followed by the resurgence of *B. burgdorferi* growth 12 months after treatment.[16] This study provides evidence that the slow-growing spirochetes that persist after treatment but are not cultivable in standard growth media may remain viable.

Inflammation of the CNS was only observed in the doxycycline-treated animals, both of which contained low numbers of morphologically intact spirochetes that were labeled solely by *B. burgdorferi*–specific, rabbit-derived polyclonal antibodies (green fluorescence) and not by monoclonal OspA antibodies. This finding is in agreement with previous observations whereby decreased OspA expression is met by reciprocal OspC up-regulation associated with transmission of spirochetes from a tick to vertebrate host.[44,45] However, this finding is contradictory to other reports that suggest OspA plays a critical role in translocating of the blood brain barrier and neuroinvasiveness.[46] With this stated, it is possible that OspA down-regulation occurs once the spirochetes have migrated beyond the blood–brain barrier into the neuropil as a means of immune evasion.

In addition to the brain of two treated animals, rare morphologically intact spirochetes immunoreactive to OspA were observed in the heart of one treated animal (IK14). Increased OspA serum titers have been reported in American patients with Lyme arthritis and indicate differential gene expression of *B. burgdorferi* dependent on tissue localization.[46,47] Furthermore, experimental studies in mice have shown enhanced OspA expression in host-adapted spirochetes during inflammation[48] and *ospA* transcription was evident posttreatment in both murine studies and our prior study in macaques.[13,49] Taken together, these findings illustrate that OspA down-regulation upon entry into mammalian hosts is reversible under certain environmental cues and support the use of polyclonal antibodies when trying to locate persistent *B. burgdorferi* spirochetes in affected tissue sections.

In this study, approximately 400 tissue sections from the experimental monkeys were examined. We identified rare spirochetes in several tissues known to be affected by LD. Although the presence of carbohydrates such as alginate,[50] typically associated with biofilms, was not evaluated with specific stains, tissues were permeabilized and then stained specifically for *B. burgdorferi*. All the spirochetes that were identified existed singly and were relatively sparse. No aggregates that would be suspected to have formed a biofilm were observed.

This is the first study in primates to comprehensively examine pathologic findings associated with the persistence of *B. burgdorferi* in the late stage of LD after antibiotic therapy. The NHP model possesses many advantages for studying human LD when compared with other animal models, including close genetic complementarity while remaining outbred (ie, approximately 93% DNA homology to humans[51]) and multiorgan involvement (ie, CNS, peripheral nervous system, heart, skeletal muscle, and joints).[52–56] Limitations from previous studies include artificial routes of inoculation (ie, needle inoculation versus the natural tick-inoculated route), high dosage of inoculum (10^7 to 10^8 spirochetes), and variable immune status of animals (ie, immunosuppressed versus immunocompetent). These limitations were abrogated in this study by use of tick inoculation in immunocompetent animals. In the late disseminated stage of infection (beyond 6 months), neither clinical signs nor indications of possible symptoms, such as reduced activity or disinterest in enrichment items, were observed by the veterinary staff. Taking into consideration that most PTLDS symptoms are subjective, it is not surprising that these were not observed or apparent, which makes it impossible for us to definitively attribute clinical relevance to the histopathologic

findings gained from this study. However, we can speculate that the minimal to moderate inflammation that was observed, especially within the CNS and peripheral nervous system, can, in part, explain the breadth of symptoms experienced by patients with late-stage LD, such as cognitive impairment and neuralgia. The clinical hallmark of early localized LD is EM, which was observed in one of the rhesus macaques from this study. However, many of the more severe chronic manifestations of LD associated with objective morbidities, such as Lyme carditis, resulting in atrioventricular blockage or sudden death, and neuroborreliosis, manifesting in nerve palsy, limb paresis, and painful radiculitis (potentially manifesting as lameness, loss of appetite, inability to jump, muscle spasms, reduced activity, and audible sounds of discomfort), have yet to be reproduced experimentally in any immunocompetent animal model.[35,57] Taking into account that LD is rarely fatal, a paucity of autopsy tissue limits opportunities to study disease pathogenesis and pathologic findings associated with natural disease. Furthermore, the rare human autopsy reports that are available represent the most severe manifestations of LD, which greatly limits our understanding of the disease spectrum. Future studies will include assessment of the ability of novel antimicrobial therapies to eliminate persistent spirochetal infection. Furthermore, this model may also be of great benefit in understanding host factors involved in the development of chronic disease after *B. burgdorferi* infection and help unravel the variable manifestations observed in human cases of LD.

Acknowledgments

We thank Dr. Peter J. Didier (Tulane National Primate Research Center, Covington, LA) for evaluation of microscopic pathologic findings and Dr. Jorge Benach (Stony Brook University School of Medicine, Stony Brook, NY) for providing CB10.

Supplemental Data

Supplemental material for this article can be found at *https://doi.org/10.1016/j.ajpath.2017.11.005*.

References

1. Steere AC, Malawista SE, Snydman DR, Shope RE, Andiman WA, Ross MR, Steele FM: Lyme arthritis: an epidemic of oligoarticular arthritis in children and adults in three Connecticut communities. Arthritis Rheum 1977, 20:7−17
2. Steere AC, Malawista SE, Hardin JA, Ruddy S, Askenase W, Andiman WA: Erythema chronicum migrans and Lyme arthritis: the enlarging clinical spectrum. Ann Intern Med 1977, 86:685−698
3. Burgdorfer W, Barbour AG, Hayes SF, Benach JL, Grunwaldt E, Davis JP: Lyme disease: a tick-borne spirochetosis? Science 1982, 216:1317−1319
4. Bacon RM, Kugeler KJ, Mead PS; Centers for Disease Control and Prevention (CDC): Surveillance for Lyme disease−United States, 1992-2006. MMWR Surveill Summ 2008, 57:1−9
5. Stanek G, Reiter M: The expanding Lyme Borrelia complex−clinical significance of genomic species? Clin Microbiol Infect 2011, 17: 487−493
6. Hinckley AF, Connally NP, Meek JI, Johnson BJ, Kemperman MM, Feldman KA, White JL, Mead PS: Lyme disease testing by large commercial laboratories in the United States. Clin Infect Dis 2014, 59:676−681
7. Wormser GP, Dattwyler RJ, Shapiro ED, Halperin JJ, Steere AC, Klempner MS, Krause PJ, Bakken JS, Strle F, Stanek G, Bockenstedt L, Fish D, Dumler JS, Nadelman RB: The clinical assessment, treatment, and prevention of Lyme disease, human granulocytic anaplasmosis, and babesiosis: clinical practice guidelines by the Infectious Diseases Society of America. Clin Infect Dis 2006, 43:1089−1134
8. Steere AC, Hutchinson GJ, Rahn DW, Sigal LH, Craft JE, DeSanna ET, Malawista SE: Treatment of the early manifestations of Lyme disease. Ann Intern Med 1983, 99:22−26
9. Aucott JN: Posttreatment Lyme disease syndrome. Infect Dis Clin North Am 2015, 29:309−323
10. Aucott JN, Crowder LA, Kortte KB: Development of a foundation for a case definition of post-treatment Lyme disease syndrome. Int J Infect Dis 2013, 17:e443−e449
11. Bockenstedt LK, Gonzalez DG, Haberman AM, Belperron AA: Spirochete antigens persist near cartilage after murine Lyme borreliosis therapy. J Clin Invest 2012, 122:2652−2660
12. Bolz DD, Weis JJ: Molecular mimicry to Borrelia burgdorferi: pathway to autoimmunity? Autoimmunity 2004, 37:387−392
13. Embers ME, Barthold SW, Borda JT, Bowers L, Doyle L, Hodzic E, Jacobs MB, Hasenkampf NR, Martin DS, Narasimhan S, Phillippi-Falkenstein KM, Purcell JE, Ratterree MS, Philipp MT: Persistence of Borrelia burgdorferi in rhesus macaques following antibiotic treatment of disseminated infection. PLoS One 2012, 7:e29914
14. Bockenstedt LK, Mao J, Hodzic E, Barthold SW, Fish D: Detection of attenuated, noninfectious spirochetes in Borrelia burgdorferi-infected mice after antibiotic treatment. J Infect Dis 2002, 186:1430−1437
15. Hodzic E, Feng S, Holden K, Freet KJ, Barthold SW: Persistence of Borrelia burgdorferi following antibiotic treatment in mice. Antimicrob Agents Chemother 2008, 52:1728−1736
16. Hodzic E, Imai D, Feng S, Barthold SW: Resurgence of persisting non-cultivable Borrelia burgdorferi following antibiotic treatment in mice. PLoS One 2014, 9:e86907
17. Straubinger RK, Summers BA, Chang YF, Appel MJ: Persistence of Borrelia burgdorferi in experimentally infected dogs after antibiotic treatment. J Clin Microbiol 1997, 35:111−116
18. Muehlenbachs A, Bollweg BC, Schulz TJ, Forrester JD, DeLeon Carnes M, Molins C, Ray GS, Cummings PM, Ritter JM, Blau DM, Andrew TA, Prial M, Ng DL, Prahlow JA, Sanders JH, Shieh WJ, Paddock CD, Schriefer ME, Mead P, Zaki SR: Cardiac tropism of Borrelia burgdorferi: an autopsy study of sudden cardiac death associated with Lyme carditis. Am J Pathol 2016, 186:1195−1205
19. Committee for the Update of the Guide for the Care and Use of Laboratory Animals; National Research Council: Guide for the Care and Use of Laboratory Animals: Eighth Edition. Washington, DC, National Academies Press, 2011.
20. Indest KJ, Howell JK, Jacobs MB, Scholl-Meeker D, Norris SJ, Philipp MT: Analysis of Borrelia burgdorferi vlsE gene expression and recombination in the tick vector. Infect Immun 2001, 69: 7083−7090
21. Embers ME, Grasperge BJ, Jacobs MB, Philipp MT: Feeding of ticks on animals for transmission and xenodiagnosis in Lyme disease research. J Vis Exp 2013, 78:50617
22. Embers ME, Hasenkampf NR, Barnes MB, Didier ES, Philipp MT, Tardo AC: Five-antigen fluorescent bead-based assay for diagnosis of Lyme disease. Clin Vaccine Immunol 2016, 23:294−303
23. Embers ME, Hasenkampf NR, Embers DG, Doyle LA: Pharmacokinetic analysis of oral doxycycline in rhesus macaques. J Med Primatol 2013, 42:57−61

24. Embers ME, Hasenkampf NR, Jacobs MB, Tardo AC, Doyle-Meyers LA, Philipp MT, Hodzic E: Variable manifestations, diverse seroreactivity and post-treatment persistence in non-human primates exposed to Borrelia burgdorferi by tick feeding. PLoS One 2017, 12: e0189071
25. Ramesh G, Didier PJ, England JD, Santana-Gould L, Doyle-Meyers LA, Martin DS, Jacobs MB, Philipp MT: Inflammation in the pathogenesis of Lyme neuroborreliosis. Am J Pathol 2015, 185: 1344–1360
26. Embers ME, Liang FT, Howell JK, Jacobs MB, Purcell JE, Norris SJ, Johnson BJ, Philipp MT: Antigenicity and recombination of VlsE, the antigenic variation protein of Borrelia burgdorferi, in rabbits, a host putatively resistant to long-term infection with this spirochete. FEMS Immunol Med Microbiol 2007, 50:421–429
27. Ramesh G, Borda JT, Dufour J, Kaushal D, Ramamoorthy R, Lackner AA, Philipp MT: Interaction of the Lyme disease spirochete Borrelia burgdorferi with brain parenchyma elicits inflammatory mediators from glial cells as well as glial and neuronal apoptosis. Am J Pathol 2008, 173:1415–1427
28. Wang F, Flanagan J, Su N, Wang LC, Bui S, Nielson A, Wu X, Vo HT, Ma XJ, Luo Y: RNAscope: a novel in situ RNA analysis platform for formalin-fixed, paraffin-embedded tissues. J Mol Diagn 2012, 14:22–29
29. Schwan TG, Burgdorfer W, Schrumpf ME, Karstens RH: The urinary bladder, a consistent source of Borrelia burgdorferi in experimentally infected white-footed mice (Peromyscus leucopus). J Clin Microbiol 1988, 26:893–895
30. Marques A: Chronic Lyme disease: a review. Infect Dis Clin North Am 2008, 22:341–360, vii-viii
31. Berende A, ter Hofstede HJ, Vos FJ, van Middendorp H, Vogelaar ML, Tromp M, van den Hoogen FH, Donders AR, Evers AW, Kullberg BJ: Randomized trial of longer-term therapy for symptoms attributed to Lyme disease. N Engl J Med 2016, 374: 1209–1220
32. Kaplan RF, Trevino RP, Johnson GM, Levy L, Dornbush R, Hu LT, Evans J, Weinstein A, Schmid CH, Klempner MS: Cognitive function in post-treatment Lyme disease: do additional antibiotics help? Neurology 2003, 60:1916–1922
33. Klempner MS, Hu LT, Evans J, Schmid CH, Johnson GM, Trevino RP, Norton D, Levy L, Wall D, McCall J, Kosinski M, Weinstein A: Two controlled trials of antibiotic treatment in patients with persistent symptoms and a history of Lyme disease. N Engl J Med 2001, 345:85–92
34. Bugrysheva JV, Godfrey HP, Schwartz I, Cabello FC: Patterns and regulation of ribosomal RNA transcription in Borrelia burgdorferi. BMC Microbiol 2011, 11:17
35. Lazarus JJ, McCarter AL, Neifer-Sadhwani K, Wooten RM: ELISA-based measurement of antibody responses and PCR-based detection profiles can distinguish between active infection and early clearance of Borrelia burgdorferi. Clin Dev Immunol 2012, 2012:138069
36. Dotevall L, Hagberg L: Penetration of doxycycline into cerebrospinal fluid in patients treated for suspected Lyme neuroborreliosis. Antimicrob Agents Chemother 1989, 33:1078–1080
37. Philipp MT, Aydintug MK, Bohm RP Jr, Cogswell FB, Dennis VA, Lanners HN, Lowrie RC Jr, Roberts ED, Conway MD, Karacorlu M: Early and early disseminated phases of Lyme disease in the rhesus monkey: a model for infection in humans. Infect Immun 1993, 61: 3047–3059
38. Karlsson M, Hammers-Berggren S, Lindquist L, Stiernstedt G, Svenungsson B: Comparison of intravenous penicillin G and oral doxycycline for treatment of Lyme neuroborreliosis. Neurology 1994, 44:1203–1207
39. Jackson CR, Boylan J, Frye JG, Gherardini FC: Evidence of a conjugal erythromycin resistance element in the Lyme disease spirochete Borrelia burgdorferi. Int J Antimicrob Agents 2007, 30:496–504
40. Caskey JR, Embers ME: Persister development by Borrelia burgdorferi populations in vitro. Antimicrob Agents Chemother 2015, 59: 6288–6295
41. Sharma B, Brown AV, Matluck NE, Hu LT, Lewis K: Borrelia burgdorferi, the causative agent of Lyme disease, forms drug-tolerant persister cells. Antimicrob Agents Chemother 2015, 59:4616–4624
42. Montgomery RR, Schreck K, Wang X, Malawista SE: Human neutrophil calprotectin reduces the susceptibility of Borrelia burgdorferi to penicillin. Infect Immun 2006, 74:2468–2472
43. Cabello FC, Godfrey HP, Bugrysheva JV, Newman SA: Sleeper cells: the stringent response and persistence in the Borreliella (Borrelia) burgdorferi enzootic cycle. Environ Microbiol 2017, 19:3846–3862
44. Schwan TG, Piesman J, Golde WT, Dolan MC, Rosa PA: Induction of an outer surface protein on Borrelia burgdorferi during tick feeding. Proc Natl Acad Sci U S A 1995, 92:2909–2913
45. Schwan TG, Piesman J: Temporal changes in outer surface proteins A and C of the Lyme disease-associated spirochete, Borrelia burgdorferi, during the chain of infection in ticks and mice. J Clin Microbiol 2000, 38:382–388
46. Pulzova L, Kovac A, Mucha R, Mlynarcik P, Bencurova E, Madar M, Novak M, Bhide M: OspA-CD40 dyad: ligand-receptor interaction in the translocation of neuroinvasive Borrelia across the blood-brain barrier. Sci Rep 2011, 1:86
47. Li X, Strle K, Wang P, Acosta DI, McHugh GA, Sikand N, Strle F, Steere AC: Tick-specific borrelial antigens appear to be upregulated in American but not European patients with Lyme arthritis, a late manifestation of Lyme borreliosis. J Infect Dis 2013, 208:934–941
48. Crowley H, Huber BT: Host-adapted Borrelia burgdorferi in mice expresses OspA during inflammation. Infect Immun 2003, 71: 4003–4010
49. Barthold SW, Hodzic E, Imai DM, Feng S, Yang X, Luft BJ: Ineffectiveness of tigecycline against persistent Borrelia burgdorferi. Antimicrob Agents Chemother 2010, 54:643–651
50. Sapi E, Balasubramanian K, Poruri A, Maghsoudlou JS, Socarras KM, Timmaraju AV, Filush KR, Gupta K, Shaikh S, Theophilus PAS, Luecke DF, MacDonald A, Zelger B: Evidence of in vivo existence of Borrelia Biofilm in Borrelial lymphocytomas. Eur J Microbiol Immunol (Bp) 2016, 6:9–24
51. Rhesus Macaque Genome Sequencing and Analysis Consortium, Gibbs RA, Rogers J, Katze MG, Bumgarner R, Weinstock GM, et al: Evolutionary and biomedical insights from the rhesus macaque genome. Science 2007, 316:222–234
52. Cadavid D, O'Neill T, Schaefer H, Pachner AR: Localization of Borrelia burgdorferi in the nervous system and other organs in a nonhuman primate model of Lyme disease. Lab Invest 2000, 80: 1043–1054
53. Cadavid D, Bai Y, Dail D, Hurd M, Narayan K, Hodzic E, Barthold SW, Pachner AR: Infection and inflammation in skeletal muscle from nonhuman primates infected with different genospecies of the Lyme disease spirochete Borrelia burgdorferi. Infect Immun 2003, 71:7087–7098
54. Cadavid D, Bai Y, Hodzic E, Narayan K, Barthold SW, Pachner AR: Cardiac involvement in non-human primates infected with the Lyme disease spirochete Borrelia burgdorferi. Lab Invest 2004, 84: 1439–1450
55. Bai Y, Narayan K, Dail D, Sondey M, Hodzic E, Barthold SW, Pachner AR, Cadavid D: Spinal cord involvement in the nonhuman primate model of Lyme disease. Lab Invest 2004, 84:160–172
56. Barthold SW, Cadavid D, Philipp MT. Animal models of Borreliosis. Edited by Radolf JD, Samuels DS. Norfolk, UK: Caister Academic Press, 2010. pp. xii, 547
57. Pachner AR, Delaney E, O'Neill T, Major E: Inoculation of nonhuman primates with the N40 strain of Borrelia burgdorferi leads to a model of Lyme neuroborreliosis faithful to the human disease. Neurology 1995, 45:165–172